Collective dynamics of two-species Bose-Einstein-condensate mixtures in a double-well potential

Haibo Qiu,[1,2,3] Jing Tian,[1] and Li-Bin Fu[1,2,*]

[1]*Institute of Theoretical Physics, Lanzhou University, Lanzhou 730000, People's Republic of China*

[2]*Institute of Applied Physics and Computational Mathematics, Beijing 100088, People's Republic of China*

[3]*Department of Physics, University of Science and Technology Beijing 100083, People's Republic of China*

(Received 12 November 2009; published 15 April 2010)

By employing a binary mixture of Bose-Einstein condensates in a symmetric double-well potential we study the collective dynamics of a two-coupled-Hamiltonian system. There we find three interesting collective dynamic regimes. Besides measure synchronization, phase synchronization and nonlocal measure synchronization have been found. We demonstrate that by varying the interspecies interaction strength, the transitions between different regimes can be found clearly. A diagram of dynamic regimes with experimentally adjustable parameters has also been presented.

DOI: 10.1103/PhysRevA.81.043613 PACS number(s): 03.75.Mn, 05.45.Xt, 05.45.Pq, 45.20.Jj

I. INTRODUCTION

Ultracold atoms are an appealing system for the study of interesting physical phenomena relevant to a variety of fields. By using this widely tunable and well-controlled system, many iconic condensed-matter systems have been realized, including the Mott-superfluid phase transition [1], Anderson localization [2], and realization of the Tonks gas [3]. The Bose-Einstein condensates (BEC) is naturally a nonlinear system, and the realization of BEC also opens new possibilities for the investigation of interesting nonlinear effects. Achievements in manipulation of BEC in double-well potentials [4] offer us a very well-controlled experiment setup to investigate the nonlinear phenomena of coupled oscillators. The dynamics of one-species BEC trapped in a double-well potential is described by a nonlinear oscillator and has been extensively studied. Loading a two-species BEC mixture in a double-well potential, due to the interspecies interaction, will provide us with a system for investigating the dynamic behavior of two coupled nonlinear oscillators.

The coupled dynamical system with oscillatory oscillation has been known as the basic ingredient in modeling emergence behavior in nature, with much work having been done in past decades [5]. Most of the previous research has concentrated on coupled dissipative systems, which would show collective synchrony, as has been demonstrated by the famous Huygens pendulum clocks [6]. However, research on coupled Hamiltonian systems is still in a primitive stage due to the complicated nature of its dynamics and the lack of a practical physical system to demonstrate its behaviors. Due to the conservation of its phase space, the dynamics' behaviors would be multifarious and show more interesting correlated behaviors [7].

Measure synchronization (MS) [8] is one of the most interesting correlated effects that have been found in coupled Hamiltonian systems. As demonstrated in Ref. [8], by increasing the coupling strength, a two-coupled-Hamiltonian system experiences a phase transition from a state in which the two-Hamiltonian systems visit different phase-space domains to a state in which the two Hamiltonian systems cover an identical phase-space domain. Unlike the original concept of synchronization in time coincidence where synchronized systems have the same evolution trajectories, there the two-Hamiltonian systems become synchronized in the sense of spatial coincidence and the synchronized systems have an identical invariant measure [8]. This concept has been extended, and partial MS and chaotic MS also have been found [9,10].

In this article, we study the collective dynamics of two-species BEC mixtures trapped in a symmetric double-well potential. This is a coupled-Hamiltonian system in semiclassical theory, for which the dynamics of each subsystem (each species) is well described by a classical Hamiltonian. For such a practical physical system we find three interesting collective dynamic regimes. Besides MS, we also find phase synchronization (PS) and nonlocal measure synchronization (NLMS). We demonstrate that by varying the interspecies interaction strength, the coherent transitions between different regimes can be found clearly. We draw the diagram of dynamic regimes with experimentally adjustable parameters. The article will be organized as follows. In Sec. II we introduce our model Hamiltonian. Section III describes the dynamics of coupled Hamiltonian systems. Section IV gives an analysis of the collective behavior. The conclusion is given in Sec. V.

II. MODEL HAMILTONIAN

By considering a two-species BEC mixture trapped in a symmetric double well, with the well-known two-mode approximation [11], the Hamiltonian can be written in a second quantization formalism as follows:

$$\begin{aligned}\hat{H} = {} & \frac{u_a}{2N_a}[(a_L^\dagger a_L)^2 + (a_R^\dagger a_R)^2] + \frac{u_b}{2N_b}[(b_L^\dagger b_L)^2 + (b_R^\dagger b_R)^2] \\ & - \frac{v_a}{2}(\hat{a}_L^\dagger \hat{a}_R + \hat{a}_R^\dagger \hat{a}_L) - \frac{v_b}{2}(b_L^\dagger b_R + b_R^\dagger b_L) \\ & + \frac{u_{ab}}{\sqrt{N_a N_b}}(a_L^\dagger a_L b_L^\dagger b_L + a_R^\dagger a_R b_R^\dagger b_R), \end{aligned} \tag{1}$$

where $\hat{a}_{L(R)}^\dagger$ ($\hat{a}_{L(R)}$) and $\hat{b}_{L(R)}^\dagger$ ($\hat{b}_{L(R)}$) are the creation (annihilation) operators for the localized modes in the left (L) or right (R) well of different species (a or b), respectively,

*lbfu@iapcm.ac.cn

and $N_{a,b}$ are the particle numbers for each species; $u_\sigma = (4\pi\hbar a_\sigma N_\sigma/m_\sigma)\int|\varphi_\sigma|^4 dr$, and $u_{ab} = 2\pi\hbar a_{ab}\sqrt{N_a N_b}(\frac{1}{m_a} + \frac{1}{m_b})\int|\varphi_a|^2|\varphi_b|^2 dr$ denote the effective interaction of atomic collision between the same kind of species and between the different species, respectively, with $\sigma = a, b$ as the indication of the species. $v_\sigma = \int[(\hbar^2/2m_\sigma)\nabla\varphi_L\nabla\varphi_R + V(r)\varphi_L\varphi_R]dr$ is the effective Rabi frequency describing the coupling between two wells. Under the semiclassical limit [11,12], the dynamics of the system can be described by a classical Hamiltonian $H = \langle\Psi_{GP}|\hat{H}|\Psi_{GP}\rangle/N$, in which $|\Psi_{GP}\rangle = \frac{1}{\sqrt{N_a!}}(\alpha_L\hat{a}_L^\dagger + \alpha_R\hat{a}_R^\dagger)^{N_a}|0,0\rangle \bigotimes \frac{1}{\sqrt{N_b!}}(\beta_L\hat{b}_L^\dagger + \beta_R\hat{b}_R^\dagger)^{N_b}|0,0\rangle$ is the collective state of the N-particle system with $N = N_a + N_b$. Here, $\alpha_j = |\alpha_j|e^{i\theta_{aj}}$ and $\beta_j = |\beta_j|e^{i\theta_{bj}}$ ($j = L$ or R) are four c numbers which correspond to the probability amplitudes of the two different species of atoms in the two wells. And the conservation of particle numbers of each species requires $|\alpha_L|^2 + |\alpha_R|^2 = 1$, $|\beta_L|^2 + |\beta_R|^2 = 1$. By introducing the relative population difference, $S_a = (|\alpha_L|^2 - |\alpha_R|^2)$, $S_b = (|\beta_L|^2 - |\beta_R|^2)$, and the relative phase difference, $\theta_\sigma = \theta_{\sigma L} - \theta_{\sigma R}$, we obtain the mean-field Hamiltonian [13]

$$H = H_a + H_b + H_{\rm int}, \tag{2}$$

with the Hamiltonian

$$H_\sigma = -\frac{u_\sigma}{2}S_\sigma^2 + v\sqrt{1 - S_\sigma^2}\cos\theta_\sigma \quad (\sigma = a, b) \tag{3}$$

and the coupling term

$$H_{\rm int} = -u_{ab}S_aS_b. \tag{4}$$

It is clearly shown that the coupling term is due to the interspecies interaction. Here we consider two species that have identical dynamical property and particle numbers, i.e., $v_a = v_b = v$,$u_a = u_b = u$.

III. DYNAMICS OF COUPLED HAMILTONIAN SYSTEMS

The dynamics of the coupled Hamiltonian system can be derived by computing $\dot{\theta} = \frac{\partial H}{\partial S}$, $\dot{S} = -\frac{\partial H}{\partial\theta}$. Then we get the motion of state which governed the dynamic evolution of the classical Hamiltonian system:

$$\dot{\theta_\sigma} = -u_\sigma S_\sigma - \frac{vS_\sigma}{\sqrt{1 - S_\sigma^2}}\cos\theta_\sigma - u_{\sigma\bar{\sigma}}S_{\bar{\sigma}}, \tag{5}$$

$$\dot{S_\sigma} = v\sqrt{1 - S_\sigma^2}\sin\theta_\sigma. \tag{6}$$

Our Hamiltonian system has two degrees of freedom (2DOF) with coordinates (S_1,θ_1) and (S_2,θ_2), therefore, the corresponding phase space is four dimensional. We are interested in showing the effects of coupling on the individual dynamics of each species; hence, the collective motions are shown by projecting the state of full system onto each element space, i.e., we study the two trajectories $[S_i(t),\theta_i(t)]$ $(i = 1,2)$ on the phase plane (S,θ).

Previous investigations on nonlinear dynamics of one species described by the classical Hamiltonian H_σ show that there would be two distinct dynamic regimes: the Josephson oscillation regime (0 phase mode) and the self-trapping regime

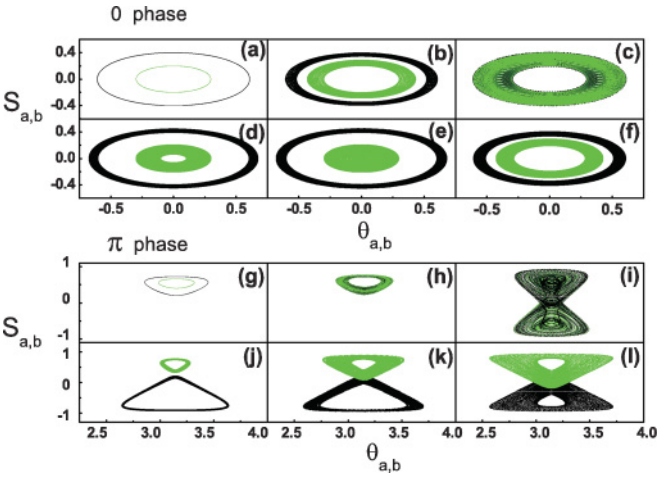

FIG. 1. (Color online) Graph of phase-space trajectories in the 0 phase mode [(a)–(f)] and the π phase mode [(g)–(l)], with initial conditions $(S_a,\theta_a,S_b,\theta_b)$ taken to be (0.2, 0.0, 0.4, 0.0) and (0.2, π, 0.4, π), respectively. (a) In the 0 phase mode with $u_{ab} = 0$, the two phase-space trajectories cover regions of two contour lines. (b) $u_{ab} = 0.008$: the two phase-space trajectory regions have begun to approach each other. (c) $u_{ab} = 0.0088$: two phase trajectories sharing the same phase-space region show that MS is achieved. (d) $u_{ab} = -0.01$: the two phase trajectory regions move in the opposite direction. (e) $u_{ab} = -0.0325$, the region of the inner phase trajectories covers the center of the phase diagram. (f) $u_{ab} = -0.07$: the two phase trajectory regions approach each other. (g) In the π phase mode with $u_{ab} = 0$, again there are two contour lines. (h) $u_{ab} = -0.0123$: two phase trajectories sharing the same phase-space region show that MS is achieved. (i) $u_{ab} = -0.075$: subsystems show chaotic behavior. (j) $u_{ab} = -0.122$: a new configuration emerges, with the two phase-space trajectory regions totally separate from each other. (k) $u_{ab} = -0.180$: the two separated phase-space trajectory regions are evolving to have a more comparable volume. (l) $u_{ab} = -0.184$: nonlocal MS is reached.

(π phase mode) with a strong nonlinearity ($u/v > 1$). To show the coupled dynamical behavior, we will discuss cases with initial conditions in the 0 phase mode and the π phase mode, respectively. Moreover, with u_{ab} denoting the interspecies interaction, one could choose either the repulsive or attractive interaction. So our text is also divided into discussions of the two different cases. Figure 1 shows the corresponding scenarios of evolution: the upper panels for the 0 phase mode with initial configuration $(S_a,\theta_a,S_b,\theta_b)$ are (0.2, 0.0, 0.4, 0.0) and the lower panels for the π phase mode with initial configuration $(S_a,\theta_a,S_b,\theta_b)$ are $(0.2,\pi,0.4,\pi)$, with simulation parameters $u = 1.2$, $v = 1.0$.

For the repulsive interspecies interaction in the 0 phase mode, Figs. 1(a)–1(c) show its evolution scenario. With $u_{ab} = 0$ [Fig. 1(a)], the two trajectories are periodic orbits in a different energy contour determined by the chosen initial conditions. With a nonzero coupling [Fig. 1(b)], the two periodic orbits are replaced by two smooth quasiperiodic trajectories wandering in two distinctive rings. By further increasing the coupling strength, we find a critical coupling strength, $\varepsilon_c = 0.0087$, for the two well-separated rings suddenly merging into an identical ring, as phase-space trajectories of the two different

species now sharing the same region in the phase space, indicating the phenomenon of measure synchronization, as shown in Fig. 1(c). This scenario is the same as that of the usual MS [8–10], before the transition point ε_c. The coupling increases the internal border of the outer ring and the external borders of the inner ring have a tendency to approach each other, while the other two boundaries of the two rings stay fixed. Until u_{ab} reaches ε_c, the two borders of the two different rings touch. Right after u_{ab} exceeds ε_c, a sudden change occurs in which the two rings cover an identical ring in phase space, which indicates the occurrence of MS. For coupling strength larger than ε_c, MS is maintained, and the shape of the identical ring will not change.

For attractive interspecies interaction in the 0 phase mode, its evolution process is shown in Figs. 1(a) and 1(d)–1(f). We find that by increasing the coupling strength, the two rings first evolve in opposite directions [Fig. 1(d)], with the internal border of the inner ring having a tendency to approach the center of the phase space while the external border of the outer ring expands. Until $u_{ab} = -0.0325$, the internal border of the inner ring finally reaches the center region while the the external border of the outer ring stops expanding [Fig. 1(e)]. Then, as the coupling strength further increases, the two rings start approaching each other until they closely touch at the transition point for MS. In this case, unlike the usual MS scenario shown earlier, we find the two rings first have a tendency to separate from each other instead of heading their way straight to the synchronized state. Nevertheless, the final MS state still covers the same spatial regions as in the previous scenario [Fig. 1(c)]. Also, we note that as coupling further increases, MS is maintained.

In the π phase mode, the dynamics are much more complicated. The most interesting finding is shown in the lower two panels of Fig. 1, which shows the case of the evolution scenario for attractive interspecies interaction. There we find the usual MS scenario: With $|u_{ab}|$ increasing, the two separate phase-space regions approach each other until u_{ab} reaches the critical coupling strength $\varepsilon_c = -0.0122$, with the two phase-space regions touching and then MS occurring [Figs. 1(g)–1(h)]. However, by further increasing the coupling strength, we find MS breakout with the emergence of chaos after u_{ab} reaches -0.0351, then as $|u_{ab}|$ further increases, new phenomena appear after the system crosses this chaotic regime [Fig. 1(i)]. Now the two phase trajectory regions suddenly separate from each other, with the original inner orbits on top of each other [Fig. 1(j)]. This corresponds to an interesting physical change: Two species initially trapped in the same well are separated and trapped in different wells when the attractive interspecies interaction strength grows larger than a critical value. After this sudden change, by further increasing u_{ab}, a new kind of collective dynamic behavior will be reached [Figs. 1(j)–1(l)], with the phase trajectory region of each species symmetrically lying on both sides of the line $S_\sigma = 0$ and covering the same acreage in phase space. This is an alternate kind of synchronization behavior, since the trajectories of subsystems also cover the same acreage but in different regions of phase space; we denote it as NLMS. We can see that in the π phase mode, besides the usual MS transition, the NLMS transition also emerges. And for the NLMS transition, unlike the MS in the 0 phase mode, the phase-space regions of the MS state would be expanded with u_{ab} further increasing.

IV. PHASE DIAGRAM OF DYNAMICAL REGIMES

The critical behaviors can be studied by introducing the so-called orbit's phase $\psi(t+dt) = \arctan\left[\frac{\theta(t+dt)-\theta(t)}{S(t+dt)-S(t)}\right]$ of each of the subsystems in phase plane (S,θ) [8]. Let $\phi(t+dt) = \psi(t+dt) + 2\pi m(t+dt)$, and let $m(t)$ be an integer which is determined as follows: If $\psi(t+dt) < \psi(t)$, $m(t+dt) = m(t)+1$; otherwise $m(t+dt) = m(t)$, and $m(0) = 0$. Because the orbits of different species have different main frequencies, $\phi(t)$ should on average vary linearly with time i.e., $\phi(t) \approx \eta t + \phi_0$ with $\eta = \lim_{t\to\infty} |\frac{\phi(t)}{t}|$ as the order parameter for the coupled Hamiltonian systems. If η is zero, it means the two orbits have the same frequencies on average; we denote this phenomenon PS. The authors of Ref. [8] found that η will decrease logarithmically to zero when coupled Hamiltonian systems reach MS (i.e., PS and MS will occur at the same time).

In Figs. 2(a) and 2(c) we plot η versus u_{ab} for the 0 phase mode and the π phase mode, respectively. For the 0 phase mode with a repulsive coupling interaction, η decreases logarithmically as u_{ab} approaches the critical point of MS and shows the same scaling behavior with what has been found by Hampton *et al.* [8]. However, with an attractive coupling interaction, things are different. For this case, η abruptly drops to zero before u_{ab} reaches the critical points of the MS transition. A closer look at the phase-space trajectories shows that the sudden drop happens at the moment when the inner

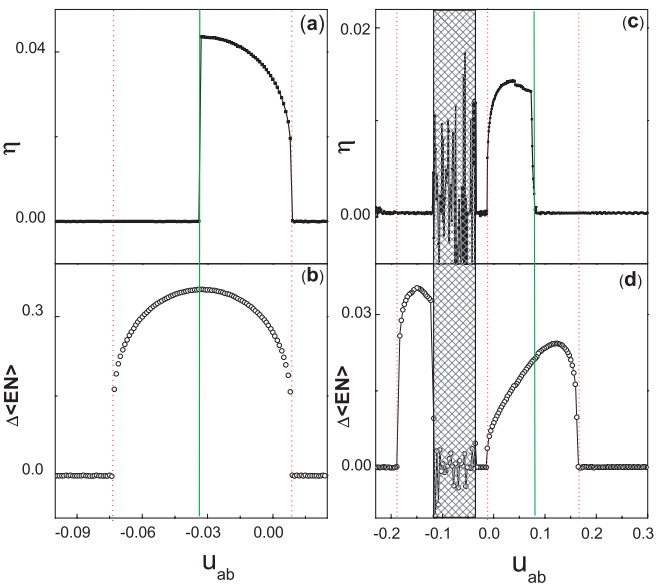

FIG. 2. (Color online) The red dotted line marks the MS transition point, and the green solid line marks the PS transition point. (a) η versus u_{ab} for the 0 phase mode. (b) The average energy difference of the two subsystems versus the coupling constant u_{ab} in the 0 phase mode. MS happens at the sharp jumps of $\Delta\langle EN\rangle$, when two average energies merge. (c) η versus u_{ab} in the π phase mode. (d) The average energy difference of the two subsystems versus the coupling constant u_{ab} in the π phase mode. MS happens at the sharp jumps of $\Delta\langle EN\rangle$, when two average energies merge.

ring begins to shrink from the center of phase space, which corresponds to Fig. 1(e).

For the π phase mode [see Fig. 2(c)], the repulsive coupling interaction case is similar to the attractive interaction case for the 0 phase mode; PS happens before MS at the moment when phase-space trajectories cover the center of phase space, with η abruptly dropping to zero. But the case for attractive coupling is quite different. At first, with increasing attractive coupling MS happens with η decreasing logarithmically at the critical point of MS (i.e., PS and MS happen simultaneously). However, there should be a chaotic regime when the trajectories cross the saddle point at $(S = 0, \theta = \pi)$. After crossing the chaotic regime the two trajectories will separate from each other, while η shows that the coupled Hamiltonian systems still preserve PS at this moment. With further increasing of the coupling strength, we will reach the NLMS.

Conclusively, we find, differing from what has been shown in previous research [8,9], that $\eta = 0$ could not be the sign for MS; it happens before MS in some cases. However, the difference between the average energies of two subsystems could be a good parameter to indicate both the MS and NLMS. For MS, the two trajectories cover the same phase-space region, so the average energies should be the same. For the NLMS, although the two phase trajectories cover different phase-space regions, the average energies are also the same. This is because, for the π phase mode, there are two symmetric dynamic regions in which the corresponding orbits have the same energy. In Figs. 2(b) and 2(d), we plot the difference of energies $\triangle\langle EN\rangle$ versus u_{ab} for the 0 phase mode and the π phase mode, respectively. We see that for MS and NLMS $\triangle\langle EN\rangle$ would be zero for both.

There are two parameters in charge of the dynamic behavior of the system that can be tuned by the Feshbach technique [14]: the interspecies interaction u_{ab} and the intraspecies interaction u. By choosing the same initial configuration for the two scenarios we have discussed, we draw its corresponding dynamic phase diagram of the two parameters in Figs. 3(a) and 3(b), respectively. For the 0 phase mode, as Fig. 3(a) shows, its diagram consists of three different dynamic regimes: the nonsynchronous state, the phase synchronized state, and the measure synchronized state. With repulsive u_{ab}, phase synchronization happens simultaneously with measure synchronization. However, with attractive coupling u_{ab}, PS happens before MS, which is marked by black in Fig. 3(a).

For the π phase mode, the diagram is much more complicated, as shown in Fig. 3(b). There now exist five different dynamic regimes. In addition to the phase synchronized state and measure synchronized state that have already been shown, two new states emerge: a nonlocal desynchronized state and a nonlocal measure synchronized state. Also, there is an unprecedented window of the system showing chaotic behavior, which we marked with a crossover line on the diagram schematically.

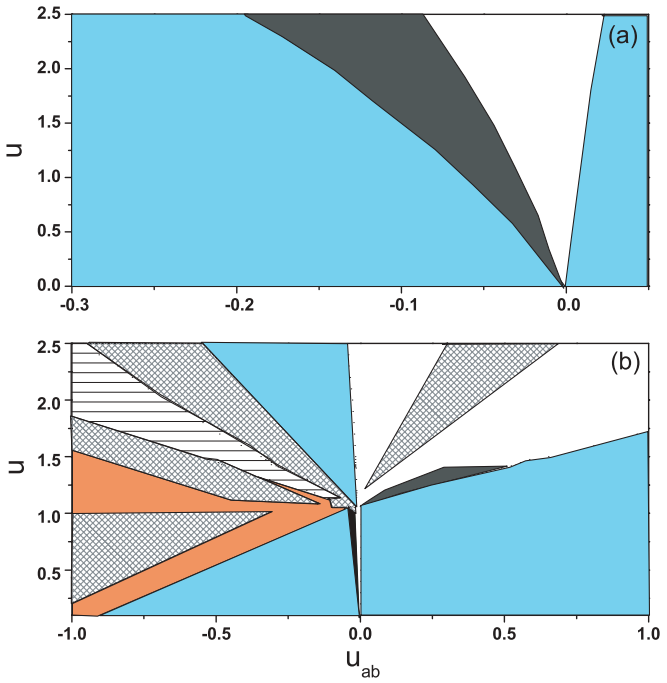

FIG. 3. (Color online) Phases as a function of interspecies and intraspecies interactions. The crossover line marks the chaotic state. Possible dynamic regimes appearing with the changing interspecies interaction include the nonsynchronized state (white), the phase synchronized state (dark) and the measure synchronized state [cyan (light gray)]. Also shown are the nonlocalized nonsynchronized state (marked by a parallel line) and the corresponding nonlocalized measure synchronized state [orange-red (dark gray)]. (a) Phase diagram in the 0 phase mode. (b) Phase diagram in the π phase mode.

V. CONCLUSION

To summarize, we have studied the collective dynamics of a two-species Bose-Einstein condensate trapped in a symmetric double-well potential. Besides MS, we also find two alternate kinds of collective dynamic regimes, the PS and NLMS. We demonstrate that by varying the interspecies interaction strength, the coherent transitions between different regimes can be found clearly. By employing an average energy difference for the characterization of the MS transition and orbit's phase difference as the order parameter of phase synchronization, we find that phase synchronization in the system always happens before MS. We draw the diagram of dynamic regimes with the experimentally adjustable parameters.

ACKNOWLEDGMENTS

We thank J. Liu for his helpful suggestions. This work was supported by the National Natural Science Foundation of China.

[1] M. Greiner, O. Mandel, T. Esslinger, T. Hänsch, and I. Bloch, Nature (London) **415**, 39 (2002).

[2] G. Roati, C. D'Errico, L. Fallani, M. Fattori, C. Fort, M. Zaccanti, G. Modugno, M. Modugno, and M. Inguscio, Nature (London) **453**, 895 (2008).

[3] B. Parades, A. Widera, V. Murg, O. Mandel, S. Fölling, I. Cirac, G. V. Schlyapnikov, T. W. Hänsch, and I. Bloch, Nature (London) **429**, 277 (2004).

[4] Y. Shin, G. B. Jo, M. Saba, T. A. Pasquini, W. Ketterle, and D. E. Pritchard, Phys. Rev. Lett. **95**, 170402 (2005); G. B. Jo, Y. Shin,

S. Will, T. A. Pasquini, M. Saba, W. Ketterle, D. E. Pritchard, M. Vengalattore, and M. Prentiss, *ibid.* **98**, 030407 (2007); M. Albiez, R. Gati, J. Fölling, S. Hunsmann, M. Cristiani, and M. K. Oberthaler, *ibid.* **95**, 010402 (2005); R. Gati, B. Hemmerling, J. Folling, M. Albiez, and M. K. Oberthaler, *ibid.* **96**, 130404 (2006).

[5] Y. Kuramoto, *Chemical Oscillations, Waves and Turbulence* (Springer, Berlin, 1984); A. Pikovsky, M. Rosenblum, and J. Kurths, *Synchronization. A Universal Concept in Nonlinear Sciences* (Cambridge University Press, Cambridge, England, 2001).

[6] C. Huygens, *Horoloquim Oscillatorium* (Paris, 1673).

[7] H. Morita and K. Kaneko, Phys. Rev. Lett. **96**, 050602 (2006).

[8] A. Hampton and D. H. Zanette, Phys. Rev. Lett. **83**, 2179 (1999).

[9] X. Wang, M. Zhan, C.-H. Lai, and H. Gang, Phys. Rev. E **67**, 066215 (2003).

[10] U. E. Vincent, New J. Phys. **7**, 209 (2005).

[11] A. Smerzi, S. Fantoni, S. Giovanazzi, and S. R. Shenoy, Phys. Rev. Lett. **79**, 4950 (1997); G. J. Milburn, J. Corney, E. M. Wright, and D. F. Walls, Phys. Rev. A **55**, 4318 (1997); R. Gati and M. K. Oberthaler, J. Phys. B **40**, R61 (2007).

[12] A. J. Leggett, Rev. Mod. Phys. **73**, 307 (2001).

[13] S. Ashhab and C. Lobo, Phys. Rev. A **66**, 013609 (2002).

[14] C. Marzok, B. Deh, C. Zimmermann, and Ph. W. Courteille, E. Tiemann, Y. V. Vanne, and A. Saenz, Phys. Rev. A **79**, 012717 (2009); S. B. Papp and C. E. Wieman, Phys. Rev. Lett. **97**, 180404 (2006); S. B. Papp, J. M. Pino, and C. E. Wieman, *ibid.* **101**, 040402 (2008); S. Inouye *et al.*, Nature (London) **392**, 151 (1998).